Received: 30 December 2019 | Revised: 5 June 2020 | Accepted: 11 June 2020
DOI: 10.1002/aoc.5913

FULL PAPER

Applied Organometallic Chemistry WILEY

Efficient One Pot Synthesis of Phenylimidazo[1,2-*a*]pyridine Derivatives using Multifunctional Copper Catalyst Supported on β-Cyclodextrin Functionalized Magnetic Graphene oxide

Saeed Bahadorikhalili[1] | **Khodadad Malek**[2] | **Mohammad Mahdavi**[3]

[1]School of Chemistry, College of Science, University of Tehran, 14155-6455, Tehran, Iran

[2]Department of Chemistry, Isfahan University of Technology, Isfahan, 84156-83111, Iran

[3]Endocrinology and Metabolism Research Center, Endocrinology and Metabolism Research Institute, Tehran University of Medical Sciences, Tehran, Iran

Correspondence
Mohammad Mahdavi, Endocrinology and Metabolism Research Center, Endocrinology and Metabolism Research Institute, Tehran University of Medical Sciences, Tehran, Iran.

Email: momahdavi@sina.tums.ac.ir

In this paper, a novel, "green", efficient and atom-economical methodology for the synthesis of *N*-(alkyl)-2-phenylimidazo[1,2-*a*]pyridin-3-amine derivatives based on copper catalyzed oxidative cyclization is presented. An efficient copper nanocatalyst was fabricated by immobilization of Cu on β-Cyclodextrin (βCD) functionalized magnetic graphene oxide nanosheets (denoted as Cu@βCD@MGO). This catalyst primarily oxidizes benzylic alcohols to aldehydes by aerobic O_2. The obtained aldehydes, in situ, takes part in a three component reaction with pyridin-2-amine and isocyanides to produce corresponding *N*-(alkyl)-2-phenylimidazo[1,2-*a*]pyridin-3-amine derivatives. The catalyst was characterized by TEM, SEM, VSM, FT-IR, XRD, TGA and ICP. As an advantage, the catalyst showed to be highly recoverable and no appreciable leaching was observed after 10 runs.

KEYWORDS
copper nanocatalyst, magnetic grapheneoxide, multifunctional catalyst, aerobic oxidation, phenylimidazopyridine

1 | INTRODUCTION

An interesting goal in clean chemistry is the development of simple synthetic methods to provide new and improved catalysts.[1–6] A large number of transition metals show catalytic activity in different transformations, while among them, copper is of importance in modern organic synthesis.[7–15] Due to the high activity and selectivity, copper catalysts have also found wide applications in several transformations such as oxidation of alcohols,[16–18] synthesis of aryl cyanides,[19,20] oxidation of carbonyl groups,[21–23] carbon-heteroatom bond formation[24,25] and 1,3-dipolar cycloaddition.[26–28]

An important issue, which has attracted great interests among researchers, is the catalyst recovery. A useful strategy is immobilization of transition metal catalysts on solid supports. By this approach, the advantage of both homogeneous and heterogeneous catalysts could be obtained to overcome the drawbacks of homogeneous transition metal catalysts.[29–33] Graphene oxide (GO) is a one-atom-thick two-dimensional sheet having honeycomb sp^2-bonded carbon. GO has attracted a great deal of interest for different potential utilizations in theoretical and experimental studies in catalysis, electronics, and material sciences.[34–36] Magnetic graphene oxide (MGO), one of the hottest materials in chemistry and material sciences, has been studied extensively due to its fantastic thermal, mechanical, and chemical properties and its unique potential technical applications.[37–42] Its remarkable characteristics such as numerous oxygen-containing groups (e.g., –OH, –COOH, and epoxy), and extremely high surface areas amenable to ligand conjugation and

https://doi.org/10.1002/aoc.5913

other manipulations enable it to be a promising candidate as a brilliant support to immobilize metal nanoparticles (NPs) for applying in catalyst development.

Among several ligands for coordination to transition metals, β-cyclodextrin is of high interest for its unique properties. Cyclodextrins are cyclic oligosaccharides of D (+)-glucopyranosyl units linked by α-1,4-glycosidic bonds and consist of a hydrophilic outer surface and a hydrophobic central cavity.[43,44] Cyclodextrins can include water-insoluble organic materials into the cavity in aqueous solution and therefore is applied in phase transfer and interface reaction catalyst.[45,46] Therefore, complexation with cyclodextrin is well-known as an effective method for enhancing dissolution properties of poorly soluble organic materials. In addition, β-cyclodextrin showed to be an appropriate ligand for copper to be applied in a 1,3-dipolar cycloaddition.[47] β-cyclodextrin is used as ligand for several metallic catalysts, including palladium,[48] copper[49] and non-metallic catalysis processes as well.[50]

Phenylimidazo[1,2-*a*]pyridine derivatives, are significant class of organic compounds and regardinig its structure, multicomponent reactions have been extended for the synthesis of this class of compounds.[51–54] We have reciently applied several nanoparticles, including superparamagnetic iron oxide mamoparticles, graphene oxide and mesoporous silica nanoparticles.[55–59] Among several nanopartices, which have been used as support for the catalysts, magnetic graphene oxide showed an advantageous benefits in the catalytic processes. For the fabrication of more efficient immobilized catalysts, β-cyclodextrin has been used as ligand in our previously published papers.[60–63] Considering the interests of the synthesis of imidazo[1,2-*a*]pyridine, in this work we focused on using Cu@BCD@MGO as a catalyst. For this purpose, we conducted oxidative, one-pot, multicomponent reaction of benzyl alcohol, isicyanides and pyridin-2-amine derivatives. Regarding our previous efforts on extending methodologies based on transition metal catalyzed reactions,[64–66] herein, we report a promising cyclization reaction methodology via aerobic alcohol oxidation using Cu catalyst decorated on polyethyleneimine modified magnetic graphene oxide to obtain corresponding *N*-methyl-2-phenylimidazo[1,2-*a*] pyridin-3-amine (**4a-j**) (Scheme 1).

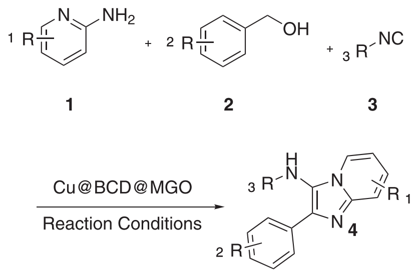

SCHEME 1 Synthesis of *N*-(alkyl)-2-phenylimidazo[1,2-*a*] pyridin-3-amine derivatives (**4a-j**)

2 | RESULTS AND DISCUSSION

The designed Cu catalyst is fabricated by immobilization of copper on βCD modified magnetic graphene oxide. For this purpose, initially, superparamagnetic graphene oxide nanosheets were synthesized and confirmed according to a previously report methods.[66] Afterwards, the magnetic graphene oxide (MGO) was manufactured from obtained GO nanosheets. MGO was synthesized by the addition of GO to a mixture containing magnetic iron oxide nanoparticles, followed by ultrasonic irradiation. Then MGO was functionalized by βCD via the covalent grafting using βCD–silane obtained from the treatment of βCD and TESPIC. The βCD@MGO was used as a dispersible pendant for immobilizing Cu nanoparticles on the surface of MGO nanosheets. Therefore, as synthesized BCD@MGO was reacted with $CuCl_2$ to provide Cu@βCD@MGO as the designed catalyst (Scheme 2). The structure of the nanocatalyst was characterized by diverse techniques including transmission electron microscopy (TEM), scanning electron microscopy (SEM), vibrating sample magnetometer (VSM), Fourier transform infrared spectroscopy (FT-IR), N_2 adsorption–desorp cvtion analysis, and inductively couple plasma-atomic emission spectrometry (ICP-AES) analysis. ICP was applied for determining the leaching of the copper after the reaction completion.

The structures of obtained nanosheets were characterized by TEM and SEM (Figure 1). The introduction of iron oxides with mean particle size of 20–25 nm onto the graphene oxide nanosheets was evident from TEM and SEM results. Iron oxide nanoparticles can be seen as dark spots within the graphene oxide nanosheets. As can be seen in Figure 1, the formation of magnetic iron oxide nanoparticles on the graphene oxide nanosheets can be clearly seen.

The magnetic behavior of the nanocatalyst was evaluated by VSM technique. The magnetic hysteresis assessed by VSM in an applied magnetic field at r.t. with the field sweeping from −8,000 to +8,000 Oe can be observed in Figure 2. The superparamagnetic nature of Cu@βCD@MGO has been shown by its S-type magnetization hysteresis loop. We note that the catalyst is magnetically recoverable. After the reaction completion, the catalyst was separated from the reaction mixture by an external magnet and reused in the next run without any additional process. For proving the presence of copper in

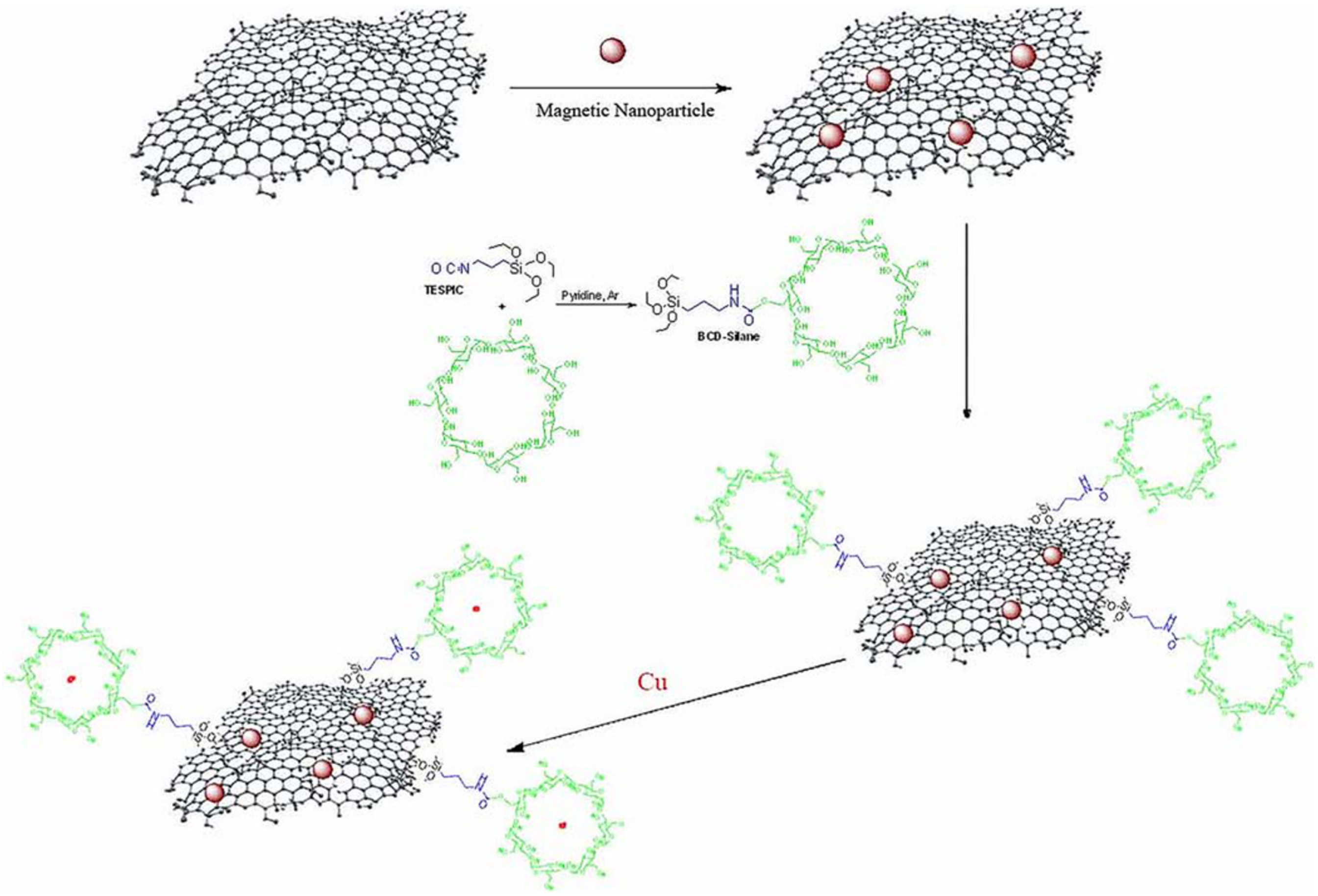

SCHEME 2 The synthesis of Cu@βCD@MGO nanocatalyst

the structure of the catalyst, EDX analysis was applied. The EDX results are presented in Figure 2b. EDX results clearly proves the presence of Cu in the strusture of Cu@βCD@MGO catalyst.

FT-IR spectroscopy was applied to prove the covalent attachment of βCD to the MGO. In the IR spectrum of GO, the strong bands at 3430 and 1,246 cm^{-1} are attributed to the stretching and bending of the O–H bond, respectively. The C=O bond in carboxylic acid (or carbonyl moieties) and aromatic C=C bond in unoxidized graphitic domains bands appeared at 1725 and 1,630 cm^{-1} respectively. The peak at 1365 cm^{-1} can be attributed to the bending absorption of carboxyl group O=C–O. The existence of Fe_3O_4 is confirmed by the appearance of the vibration band of Fe–O around 572 cm^{-1}, in the FTIR spectrum of MGO. The appearance of such bands in FTIR spectrum of βCD@MGO is in agreement with the attachment of βCD to the MGO. The bands at 3430 cm^{-1} are due to the O–H groups of βCD attached to the surface, and the band at 1691 cm^{-1} assigned to the C=O. FT-IR spectra of the nanocatalyst showed characterization peaks for Fe–O–Fe, C=O and O–H groups (Figure 3), which indicates the presence of iron oxide and graphene oxide nanosheets.

It is believed that the immobilization of pincer-like βCD pendant on the surface of MGO provides a good distribution of catalytically active Cu species on the support and accordingly it stabilizes Cu during the chemical reaction, and also prevents the aggregation of Cu nanoparticles. Moreover, the Cu content of the obtained solid catalyst was 0.25 mmol per gram of [Cu@βCD@MGO] catalyst using ICP-AES (0.016 wt%).

The structure of the catalyst was studied by XRD method. Figure 4 shows the XRD patterns of Cu@βCD@MGO. The diffraction pattern matches the desired structure of copper supported magnetic graphene oxide. In the diffraction pattern in Figure 4, an intense peaks at $2\theta = 11.4°$ could be assigned to the reflection of the 001 plates of graphene oxide. In addition, the peaks at $2\theta = 30.3°$ (220), 35.7° (311), 43.5° (400), 53.9° (422), 57.5° (511) and 63.0° (440) could be correlated to the standard XRD data of magnetic iron oxide nanoparticles. It should be noted that, the diffraction peak at $2\theta = 11.4°$ of graphene oxide is disappeared. This observation can be due to the covering up the weak carbon peaks by iron

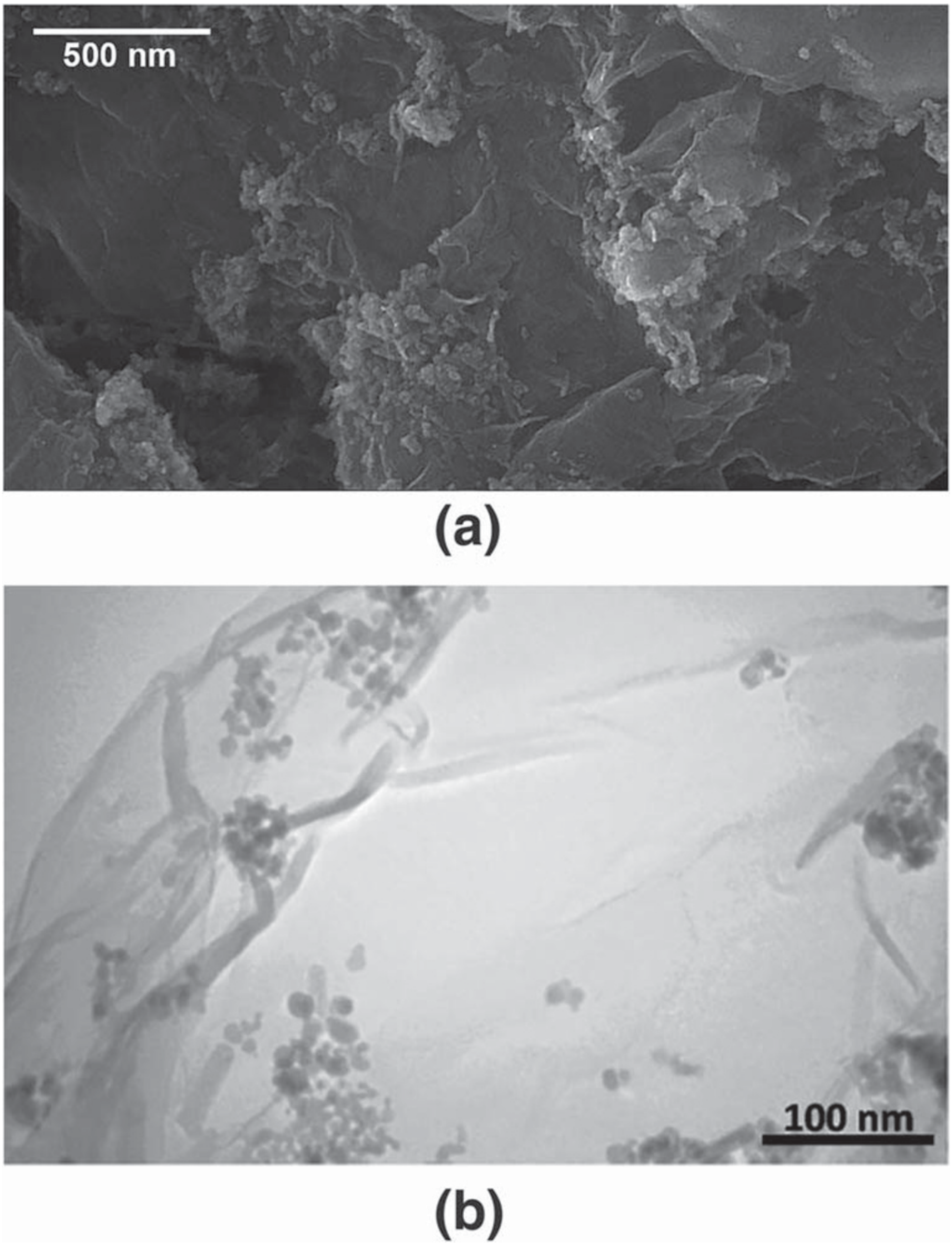

FIGURE 1 SEM (Top) and TEM images (Bottom) of Cu@βCD@MGO

oxides after functionalizing the graphene oxide by superparamagnetic iron oxide nanoparticles.[67,68]

The functionalization content in Cu@βCD@MGO catalyst was evaluated by thermogravimetric analysis (TGA) TGA result of Cu@βCD@MGO catalyst is presented in Figure 5. It could be observed that a weight loss is occurred in 100 °C, which could be correlated to the evaporation of the adsorbed water. The weight loss in higher temperatures are due to the decomposition of the organic moieties in the structure of the catalyst.

The activity of the catalyst was subsequently investigated upon characterization in the C-O oxidation followed by multicomponent reaction between the produced aldehydes, pyridin-2-amine and isocyanides (Scheme 1). The reaction was studied for finding the optimized conditions. Several factors, which affect the reaction performance, and therefore the yield of the reaction, were optimized. For this purpose, only one variable was changed and all the other variables were remained constant to see the effect of the studied variable on the reaction performance. Blank runs showed the lack of catalytic activity in the presence of MGO or βCD@MGO.

To find the optimal condition, the reaction between benzyl alcohol, pyridin-2-amine and cyclohexyl isocyanide was selected as a model reaction and was performed under different conditions. Performing the reaction in the presence of different amounts of the catalyst proved that, the high amounts of the products are formed

FIGURE 2 VSM (a) and EDX (b) result of Cu@βCD@MGO

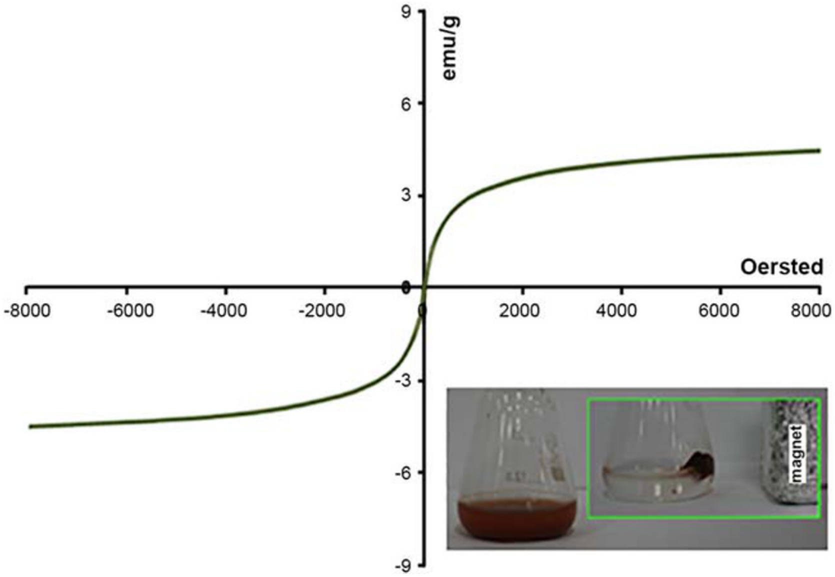

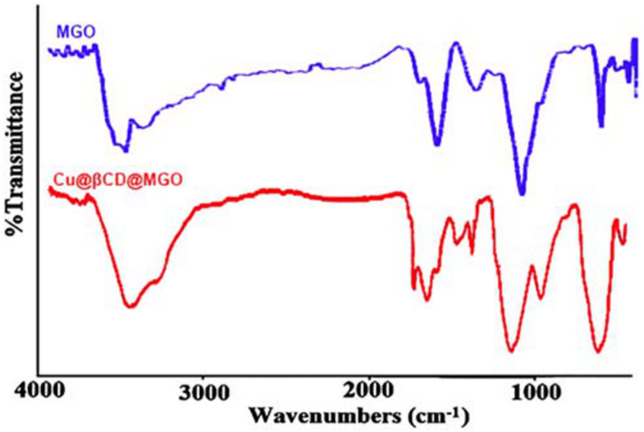

FIGURE 3 FTIR spectra for magnetic graphene oxide and Cu@βCD@MGO

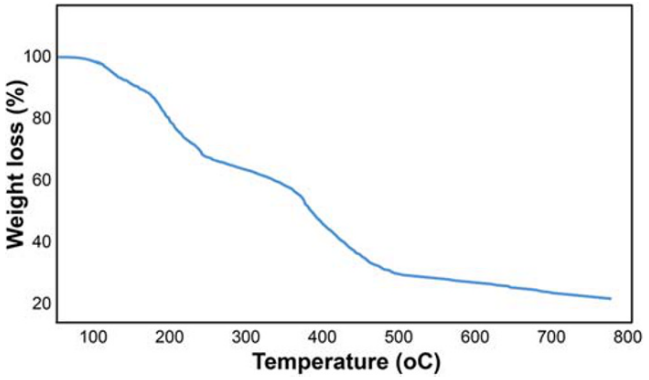

FIGURE 5 TGA curve of Cu@βCD@MGO catalyst

when 25 mg of the catalyst (0.5 mol%) is used for each mmol of the substrates after 12 hr. The results are presented in Table 1. According to the results of Table 1, the presence of the catalyst is essential for the reaction performance. It could be observed that no products was observed when the reaction as performed without the catalyst. Moreover, a reaction was performed and the catalyst was separated after 4 hr. The reaction was

FIGURE 4 XRD pattern of Cu@βCD@MGO catalyst

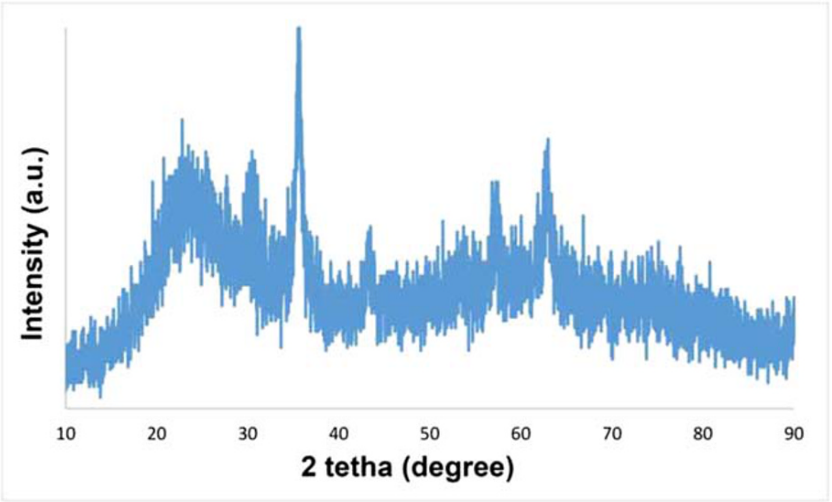

TABLE 1 Effect of the amount of catalyst on the isolated yield[a]

Entry	Catalyst (mol%)	Isolated Yield (%)
1	0.00	0
2	0.12	17
3	0.25	40
4	0.37	62
5	0.50	73
6	0.75	73
7	1.25	74
8	1.50	74
9	2.00	74

[a] Condition: 2-chlorobenzyl alcohol (1 mmol), pyridin-2-amine (1 mmol), and cyclohexyl isocyanide (1 mmol) in EtOH at 70 °C for 24 hr.

continued without the catalyst up to 12 hr. The performance of the reaction was followed by GC analysts. The results showed that after the removal of the catalyst, the reaction has not been completed.

Finally, we performed the reaction in various solvents. Table 2 shows that the product formation is observed in all the tested solvents, however the best results were observed for the reactions which have been carried out in DMSO or EtOH as solvent. Regarding the advantages of ethanol, such as environmental friendly, low toxicity, facile work up and lower cost in comparison with DMSO, ethanol was selected as the best solvent for the reaction.

We investigated the scope of the Cu catalyzed oxidative cyclization reactions between benzyl alcohol, pyridin-2-amine, and isocyanides (**4a-j**) under the optimized conditions. As shown in Table 3, the corresponding *N*-alkyl-2-phenylimidazo[1,2-*a*]pyridin-3-amine derivatives were obtained in moderate to good yields for various examined substrates at 70 °C. As illustrated, a wide range of products can be efficiently produced with this catalytic system. All substrates possessing electron-rich as well as electron-poor substituents underwent the cyclization reaction catalyzed by Cu@βCD@MGO.

TABLE 2 Effect of different solvents on the reaction time and the isolated yield[a]

Entry	Solvent	Time (hr)	Isolated Yield (%)
1	H_2O	47	41
2	DMF	36	56
3	DMSO	36	67
4	EtOH	12	73
5	EtOH	48	48
6	CH_2Cl_2	48	55
7	CH_3CN	48	41

[a] Condition: 2-chlorobenzyl alcohol (1 mmol), pyridin-2-amine (1 mmol), and cyclohexyl isocyanide (1 mmol) at 70 °C.

A great advantage of Cu@βCD@MGO is its reusability. The separation of the catalyst from the reaction mixture could simply be done by using an external magnet. For evaluating the reusability of the catalyst, the reaction of 4-methylbenzyl alcohol, cyclohexyl isocyanide and pyridin-2-amine was selected as the model reaction. The reusability study was performed under the optimized reaction conditions. After the reaction completion, the catalyst was separated by a magnet and in the next reaction. The reaction was repeated for 10 runs and no decrease in the reaction performance was observed (Figure 6).

For studying the stability of the catalyst in the reaction conditions, the structure of Cu@βCD@MGO was evaluated after recovery of the catalyst by several methods, including VSM, TGA, and ICP analysis. The results of TGA and VSM analyses of Cu@βCD@MGO catalyst after 5th cycle of recovery is presented in Figure 7a and b, respectively. It could be observed that, the characters and the properties of the catalyst has not been changed in the reaction conditions. For studying possible leaching of copper from the catalyst, Cu@βCD@MGO was recovered from the reaction mixture after the reaction completion after first and fifth cycles. The solution was analyzed by ICP-AES and no copper was observed, which proves the stability of the catalyst in the reaction conditions. This catalyst is prominent due to the efficient recoverability and high turnover number (TON). The robust catalyst achieved cumulative TONs of about 1,500 over 10 successive runs. The cumulative TON is obtained by the sum of the values for the TONs for all examined runs. In addition, the catalyst was added to the reaction solvent and stirred under the reaction conditions. After 24 h, the catalyst was separated and the solution as characterized for any possibly leaching by ICP analysis. ICP results proved no leaching of the catalyst, which shows the stability of Cu@βCD@MGO under the reaction conditions.

Regarding the good performance of the reaction in the presence of Cu@βCD@MGO, a possible mechanism was proposed, which is presented in Scheme 3. As can be seen, at the beginning of the reaction, an aerobic oxidation of benzyl alcohol to the corresponding albehyde takes place in the presence of Cu@βCD@MGO catalyst. The great advantage of this step is that the oxidation reaction occurs in the presence of the oxygen in the air and

TABLE 3 Substrate scope exploration[a]

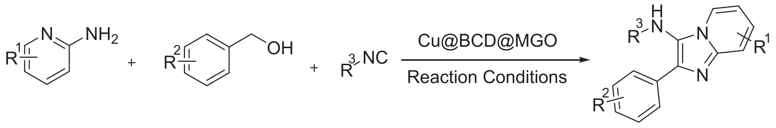

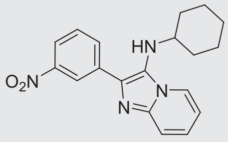

4a, 71%

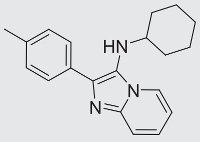

4b, 76%

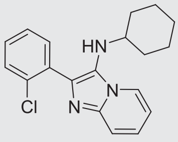

4c, 73%

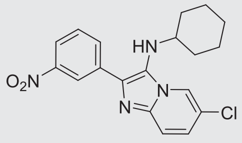

4d, 68%

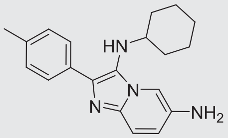

4e, 65%

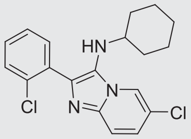

4f, 74%

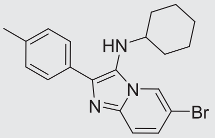

4g, 70%

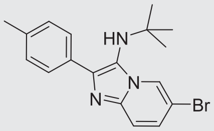

4h, 72%

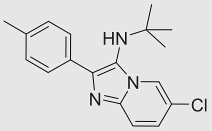

4i, 69%

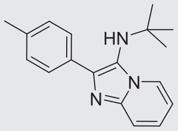

4j, 75%

[a] Condition: alcohol (1 mmol), pyridin-2-amine (1 mmol), isocyanide (1 mmol), and Cu@βCD@MGO (0.50 mol%) in ethanol at 70 °C for 12 hr.

FIGURE 6 reusability of Cu@βCD@MGO catalyst after 10 sequential runs

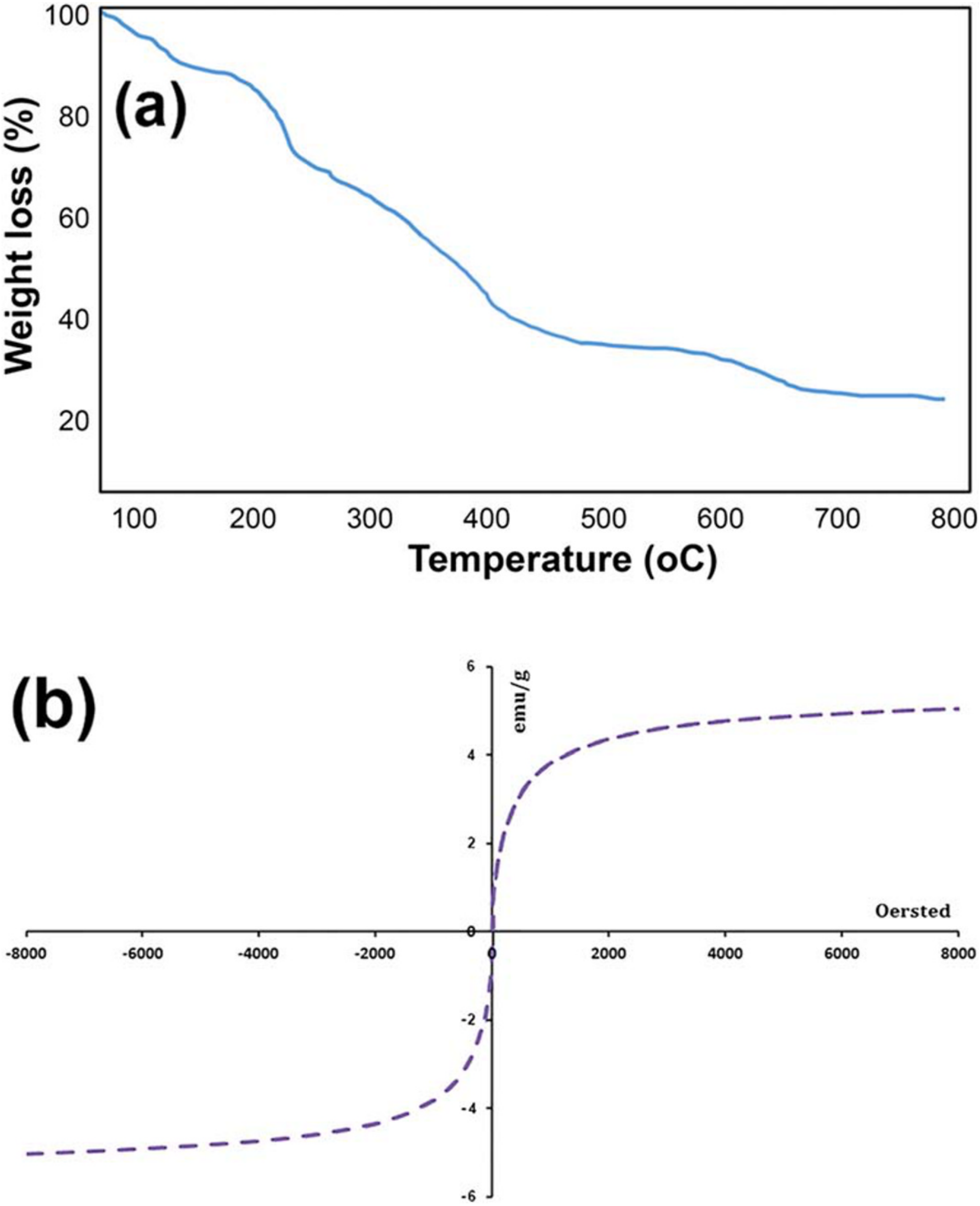

FIGURE 7 (a) TGA curve; and (b) VSM result of Cu@βCD@MGO after 5th cycle of the recovery of the catalyst

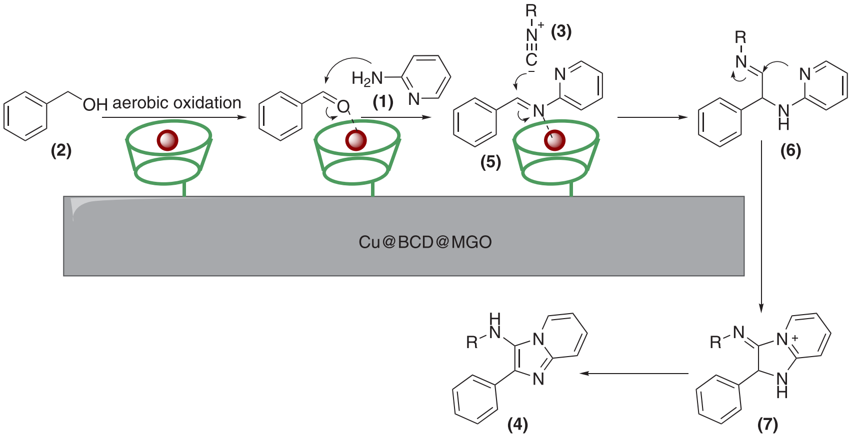

SCHEME 3 Proposed mechanism for Cu@βCD@MGO catalyzed synthesis of phenylimidazo[1,2-*a*]pyridine derivatives

there is no need to any other oxidizing reagent. The fabricated aldehyde, reacts to pyridin-2-amine and forms 1-phenyl-*N*-(pyridin-2-yl)methanimine **(5)** the reaction of 1-phenyl-*N*-(pyridin-2-yl)methanimine with isocyanide derivative leads to the formation of *N*-(2-(alkylimino)-1-phenylethyl)pyridin-2-amine **(6)**. An intramolecular cyclization reaction takes place in *N*-(2-(alkylimino)-1-phenylethyl)pyridin-2-amine, which gives 3-(alkylimino)-2-phenyl-2,3-dihydro-1*H*-imidazo[1,2-*a*]pyridin-4-ium **(7)**. The desired phenylimidazo[1,2-*a*]pyridine will be formed by a 1,3-H shift in compound **(7)**.

A comparison between the current method and previously reported methods for the synthesis of phenylimidazo[1,2-*a*]pyridine derivatives showed the good activity and high performance of Cu@βCD@MGO catalyst for the synthesis of the mentioned compounds. In most cases, the use of non-reusable catalysts limit industrial production of these compounds.[51] In addition, using toxic[51] or high temperature conditions are of other drawbacks of some of previous reports.[69] In this work, the reaction was performed in ethanol as a green and nontoxic solvent. In addition alcohols were oxidized by aerobic oxygen.

3 | CONCLUSIONS

In summary, we have introduced a novel methodology for the facile synthesis of *N*-alkyl-2-phenylimidazo[1,2-*a*]pyridin-3-amine based on Cu catalyzed C-O oxidation followed by multicomponent cyclization reactions. A novel and efficient Cu containing βCD modified magnetite graphene oxide, Cu@βCD@MGO has been developed as highly active and stable nanocatalyst for simultaneous C-O bond oxidation and multicomponent reactions. The transformation proceeded well with a broad substrate scope under mild conditions to achieve high to moderate isolated yields. The salient features of the proposed method include high efficiency, generality and simplicity which lead to high yields, a cleaner reaction profile and easy recyclability of the highly stable heterogeneous catalyst by a simple magnet separation.

4 | EXPERIMENTAL

4.1 | General remarks

Solvents, reagents and chemicals were obtained from Merck (Germany) and Fluka (Switzerland) Chemical Companies. Melting points were taken on a Kofler hot stage apparatus and are uncorrected. The IR spectra were obtained on a Nicolet Magna FT-IR 550 spectrophotometer (potassium bromide disks). Nuclear magnetic resonance spectra were recorded on a Brucker Bruker FT-500 spectrometers using tetramethylsilane (TMS) as internal standard in pure deuterated solvents. Chemical shifts are given in the δ scale in parts per million (ppm) and singlet (s), doublet (d), triplet (t), multiplet (m) and doublets of doublet (dd) are recorded. Mass spectra were recorded on an Agilent Technology (HP) mass spectrometer operating at an ionization potential of 70 eV. The elemental analysis was performed with an Elemetar Analysen system GmbH VarioEL CHNS mode. Purification of all product were conducted by column chromatography on silica gel using petroleum ether and ethyl acetate as eluent. Thin layer chromatography was carried out on silica gel 254 analytical sheets obtained from Fluka. Column chromatography was carried out on the column of silica gel 60 Merck (230–240 mesh) in glass columns (2 or 3 cm diameter) using 15–30 grams of silica gel per one gram of the crude mixture. Transition electron microscope images were recorded on a HITACHI S-4160. Thermogravimetric analysis of the samples were recorded by TGA Q50 V6.3 Build 189 instrument.

4.2 | Preparation of graphene oxide

The GO was manufactured from graphite using modified Hummer's method according to our previous report.[66] Briefly, 1 g of graphite powder was added to a continuous stirring solution of 50 mL H_2SO_4 98% in an ice bath and then, 2 g $KMnO_4$ was gently added to it. It should be noted that the rate of addition was carefully controlled to avoid a sudden increase of mixture temperature. The reaction mixture was left to stir for 2 hr at temperatures below 10 °C, and followed by another 1 hr at 35 °C. Then the reaction mixture was diluted with 50 ml of deionized water (DW) in an ice bath and the temperature was kept below 100 °C. After 1 hr of stirring, the mixture was further diluted to 150 ml with DW. Then, 10 ml of H_2O_2 30% was added to the mixture which changing its color to brilliant yellow. The resulting solid was separated by centrifuge and washed thoroughly with 5% HCl aq. solution and DW to neutralize. Finally it was dried at 60 °C for 24 hr.

4.3 | Preparation of magnetic graphene oxide (MGO)

The MGO nanosheets were synthesized by co-precipitation of Fe^{3+} and Fe^{2+} in the presence of GO.[66] The solution of Fe^{3+} and Fe^{2+} was prepared in a 2:1 mole ratio. 500 mg of GO was dispersed in 40 mL of water by sonication for 45 min. Then a 50 mL solution of $FeCl_3$ (1 g) and $FeCl_2$ (375 mg) in DW was added to the later solution. The reaction temperature was raised to 85 °C and ammonia solution 30% was added to pH 10. After 45 min of vigorously stirring, the solution was cooled to r.t., and finally the obtained black precipitate was centrifuged at 6000 rpm for 10 min and washed thoroughly with DW and dried at 60 °C for 24 hr.

4.4 | Preparation of BCD functionalized MGO

βCD-Silane was synthesized via the hydrogen-transfer nucleophilic addition reaction between the end hydroxyl group of βCD and 3-(triethoxysilyl)propyl isocyanate (TESPIC). 10 mmol of βCD was dissolved into 50 ml of dry pyridine with vigorous stirring under argon atmosphere at 70 °C. After stirring for 6 hr, 10 mmol of TESPIC was added into the later solution. After 24 h, the solvent was removed by vacuum evaporation. The residue was washed three times with *n*-hexane, and then recrystallized from EtOH.

Then a solution of 1 g of βCD–silane in 30 ml of EtOH was added drop-wise to a vigorous stirring solution of 250 mg of MGO in 30 ml EtOH/H_2O (1:2) and HCl (pH = 4). After vigorous stirring for 24 hr, the solution was magnetically separated and washed thoroughly with EtOH. The white residue was dried at 100 °C in vacuum for 12 hr to obtain βCD@MGO.

4.5 | Preparation of cu@BCD@MGO catalyst

To a mixture of βCD@MGO (1 g) in 50 ml dry CH_2Cl_2, $CuCl_2$ (2 mmol) was added and stirred at room temperature under argon atmosphere for 24 hr. The obtained solid was magnetically separated and washed with CH_2Cl_2 (2 × 10 ml) and Et_2O (2 × 10 ml). Cu@βCD@MGO nanocatalyst was obtained as a dark black powder after drying under vacuum for 12 hr.

4.6 | General procedure for cu@βCD@MGO catalyzed synthesis of *N*-alkyl-2-phenylimidazo[1,2-*a*]pyridin-3-amines

Pyridin-2-amine (0.282 g, 3 mmol), benzyl alcohol (0.324 g, 3 mmol) and cyclohexyl isocyanide (0.327 g, 3 mmol) were dissolved in 10 ml of ethanol in an open flask and 0.50 mol% (25 mg) of Cu@βCD@MGO was added. The reaction mixture was stirred at 70 °C for 12 hr. After the reaction completion, monitored by TLC, the catalyst was separated using an external magnet. The solvent was evaporated and the products were purified by recrystallization from ethanol. The structure of all compounds were confirmed by spectral data (^1H and ^{13}CNMR, FT-IR, mass spectroscopy) [See supplementary information]. The recovered catalyst was rinsed with water and EtOH, and finally dried at r.t. and reused without any pretreatment for the next run. The recycling test of the catalyst was performed in the reaction according to the above procedure.

1.1 | Recovery of cu@βCD@MGO catalyst

For studying the reusability of the catalyst, the reaction of 4-methylbenzyl alcohol, cyclohexyl isocyanide and pyridin-2-amine was selected as the model reaction. After the reaction was completed, the catalyst was separated from the reaction mixture by using an external magnet. The catalyst was used in the next reaction and this process was repeated for 10 times. Each reaction was performed in the optimal conditions, including 4-methylbenzyl alcohol (1 mmol), cyclohexyl isocyanide (1 mmol), pyridin-2-amine (1 mmol), and Cu@βCD@MGO (0.50 mol%) in ethanol for 12 hr.

ORCID

Saeed Bahadorikhalili https://orcid.org/0000-0001-8047-342X
Mohammad Mahdavi https://orcid.org/0000-0002-8007-2543

REFERENCES

[1] A. Rajendran, T. Y. Cui, H. X. Fan, Z. Yang, J. Feng, W. Li, *J. Mater. Chem. A* **2020**, *8*, 2246.
[2] R. L. Vekariya, *J. Mol. Liq.* **2017**, *227*, 44.
[3] M. Wu, L. Li, N. Liu, D. Wang, Y. Xue, L. Tang, *Process. Saf. Environ. Protect.* **2018**, *118*, 40.
[4] X. Xiong, K. M. Iris, L. Cao, D. C. Tsang, S. Zhang, Y. S. Ok, *Bioresour. Technol.* **2017**, *246*, 254.
[5] S. Seydey, M. Khalilpour, Z. Rezaei, S. S. Homami, *J. Chem. Res.* **2015**, *39*, 286.
[6] G. Rahimzadeh, S. Bahadorikhalili, E. Kianmehr, M. Mahdavi, *Mol. Diversity* **2017**, *21*, 597.
[7] K. Feher, E. Nagy, P. Szabo, T. Juzsakova, D. Sranko, A. Gomory, L. Kollar, R. Skoda-Foldes, *Appl. Organomet. Chem.* **2018**, *32*, e4343.
[8] L. Pang, J. Sun, M. Zheng, H. Li, Y. Wang, T. Zhang, *Appl. Catal. Environ.* **2019**, *254*, 510.
[9] S. Bahadorikhalili, M. Mahdavi, L. Ma'mani, A. Shafiee, H. Mahdavi, T. Akbarzadeh, *New J. Chem.* **2018**, *42*, 5499.
[10] J. Singh, G. Kaur, M. Rawat, *J. Bioelectron. Nanotechnol.* **2016**, *1*, 2.
[11] J. Zhang, E. Khaskin, N. P. Anderson, P. Y. Zavalij, A. N. Vedernikov, *Chem. Commun.* **2008**, 3625.
[12] T. W. Lyons, M. S. Sanford, *Chem. Rev.* **2010**, *110*, 1147.

[13] C. L. Bracey, P. R. Ellis, G. J. Hutchings, *Chem. Soc. Rev.* **2009**, *38*, 2231.
[14] A. Y. Mitrofanov, A. V. Murashkina, I. Martín-García, F. Alonso, I. P. Beletskaya, *Catal. Sci. Technol.* **2017**, *7*, 4401.
[15] S. Korwar, K. Brinkley, A. R. Siamaki, B. F. Gupton, K. C. Ellis, *Org. Lett.* **2015**, *17*, 1782.
[16] S. D. McCann, S. S. Shannon, *Acc. Chem. Res.* **2015**, *48*, 1756.
[17] X. Boran, J. P. Lumb, B. A. Arndtsen, *Angew. Chem. Int. Ed.* **2015**, *54*, 4208.
[18] J. Yu, Y. Luan, Y. Qi, J. Hou, W. Dong, M. Yang, G. Wang, *RSC Adv.* **2014**, *4*, 55028.
[19] T. Chuanzhou, F. Liu, Y. Zhu, W. Liu, Z. Cao, *Org. Biomol. Chem.* **2012**, *11*, 3349.
[20] G. Lijun, C. Jin, *Chem. Commun.* **2015**, *51*, 6572.
[21] W. Jing, C. Liu, J. Yuan, A. Lei, *Angew. Chem. Int. Ed.* **2012**, *52*, 2256.
[22] R. S. Kumar, S. Guin, K. K. Ghara, A. Banerjee, B. K. Patel, *Org. Lett.* **2012**, *14*, 3982.
[23] T. Conghui, N. Jiao, *Angew. Chem. Int. Ed.* **2014**, *53*, 6528.
[24] Z. Xu, S. Chiba, *Chem. Soc. Rev.* **2016**, *45*, 4504.
[25] R. Gujadhur, K. Craig, G. Bates, D. Venkataraman, *Org. Lett.* **2001**, *3*, 4315.
[26] P. E. Ana, M. G. Esguevillas, S. Padilla, J. Adrio, J. C. Carretero, *Org. Lett.* **2014**, *16*, 2228.
[27] B. T. Worrell, J. A. Malik, V. V. Fokin, *Science* **2012**, *340*, 457.
[28] R. Qiu, H. Luo, *RSC Adv.* **2015**, *5*, 96213.
[29] E. Guibal, *Prog. Polym. Sci.* **2005**, *30*, 71.
[30] Y. Wang, H. Arandiyan, J. Scott, A. Bagheri, H. Dai, R. Amal, *J. Mater. Chem. A* **2017**, *5*, 8825.
[31] R. Silbernagel, A. Díaz, E. Steffensmeier, A. Clearfield, J. Blümel, *J. Mol. Catal. A: Chem.* **2014**, *394*, 217.
[32] S. B. Khalili, A. R. Sardarian, *Monatsh. Chem.* **2012**, *143*, 841.
[33] S. Bahadorikhalili, A. R. Sardarian, *Polycycl. Aromat. Comp.* **2019**, 1. https://doi.org/10.1080/10406638.2018.1517808
[34] I. Khan, A. Ibrar, N. Abbas, A. Saeed, *Eur. J. Med. Chem.* **2014**, *76*, 193.
[35] X. Chen, Y. Du, H. Sun, F. Wang, L. Kong, M. Sun, *Bioorg. Med. Chem. Lett.* **2014**, *24*, 884.
[36] S. Bahadorikhalili, H. Mahdavi, *Polym. Adv. Technol.* **2018**, *29*, 1138.
[37] A. Sherlala, A. Raman, M. Bello, A. Asghar, *Chemosphere* **2018**, *193*, 1004.
[38] S. Hu, G. Xie, D. X. Zhang, C. Davis, W. Long, Y. Hu, F. Wang, X. Kang, F. Tan, L. Ding, Y. Wang, *Bioorg. Med. Chem. Lett.* **2012**, *22*, 6301.
[39] K. W. Fowler, D. Huang, E. A. Kesicki, H. C. Ooi, A. Oliver, F. Ruan, J. Treiberg, K. D. Puri, *US Patent* RE44599, **2013**.
[40] V. A. Glushkov, Y. V. Shklyaev, *Chem. Heterocycl. Compd.* **2001**, *37*, 663.
[41] L. P. Lingamdinne, J. R. Koduru, R. R. Karri, *J. Environment. Manag.* **2019**, *231*, 622.
[42] G. Liu, L. Li, D. Xu, X. Huang, X. Xu, S. Zheng, Y. Zhang, H. Lin, *Carbohydr. Polym.* **2017**, *175*, 584.
[43] E. M. Del Valle, *Process Biochem.* **2004**, *39*, 1033.
[44] G. Astray, C. Gonzalez-Barreiro, J. C. Mejuto, R. Rial-Otero, J. Simal-Gandara, *Food Hydrocolloids* **2009**, *23*, 631.
[45] A. Saeed, Z. Ashraf, *Pharm. Chem. J.* **2008**, *42*, 277.
[46] J. F. Guastavino, S. M. Barolo, R. A. Rossi, *Eur. J. Org. Chem.* **2006**, *17*, 3898.
[47] K.B. Simonsen, J. Kehler, K. Juhl, N. Khanzhin, S.M. Nielsen, *Patent*, WO2008131779A1, **2008**.
[48] S. Sadjadi, M. M. Heravi, M. Raja, *Carbohydr. Polym.* **2018**, *185*, 48.
[49] S. E. Sadat-Ebrahimi, S. M. Haghayegh-Zavareh, S. Bahadorikhalili, A. Yahya-Meymandi, M. Mahdavi, M. Saeedi, *Synth. Commun.* **2018**, *47*, 2324.
[50] S. Sadjadi, M. M. Heravi, M. Raja, F. G. Kahangi, *Appl. Organomet. Chem.* **2018**, *32*, e4508.
[51] E. Allahabadi, S. Ebrahimi, M. Soheilizad, M. Khoshneviszadeh, M. Mahdavi, *Tetrahedron Lett.* **2017**, *58*, 21.
[52] A. B. Ramesha, G. M. Raghavendra, K. N. Nandeesh, K. S. Rangappa, K. Mantelingu, *Tetrahedron Lett.* **2013**, *54*, 95.
[53] K. Pericherla, P. Kaswan, K. Pandey, A. Kumar, *Synthesis* **2015**, *47*, 887.
[54] A. K. Bagdi, S. Santra, K. Monir, A. Hajra, *Chem. Commun.* **2015**, *51*, 1555.
[55] S. Bahadorikhalili, S. Ansari, H. Hamedifar, L. Ma'mani, M. Babaei, R. Eqra, M. Mahdavi, *Appl. Organomet. Chem.* **2019**, *33*, e4769.
[56] M. H. Sayahi, S. Bahadorikhalili, S. J. Saghanezhad, M. A. Miller, M. Mahdavi, *Res. Chem. Intermediat.* **2020**, *46*, 491.
[57] Z. Tashrifi, S. Bahadorikhalili, H. Lijan, S. Ansari, H. Hamedifar, M. Mahdavi, *New J. Chem.* **2019**, *43*, 8930.
[58] Z. Heydari, S. Bahadorikhalili, P. Rashidi Ranjbar, M. Mahdavi, *Appl. Organomet. Chem.* **2018**, *32*, e4561.
[59] M. H. Sayahi, S. Bahadorikhalili, S. J. Saghanezhad, M. Mahdavi, *Res. Chem. Intermediat.* **2018**, *44*, 5241.
[60] S. Bahadorikhalili, S. Ansari, H. Hamedifar, M. Mahdavi, *Int. J. Biol. Macromol.* **2019**, *135*, 453.
[61] M. Mahdavi, H. Lijan, S. Bahadorikhalili, L. Ma'mani, P. Rashidi-Ranjbar, A. Shafiee, *RSC Adv.* **2016**, *6*, 28838.
[62] S. Bahadorikhalili, A. Ashtari, L. Ma'mani, P. Rashidi Ranjbar, M. Mahdavi, *Appl. Organomet. Chem.* **2018**, *32*, e4212.
[63] R. Tarasi, M. Khoobi, H. Niknejad, A. Ramazani, L. Ma'mani, S. Bahadorikhalili, A. Shafiee, *J. Magn. Magn. Mater.* **2016**, *417*, 451.
[64] S. Bahadorikhalili, L. Ma'mani, H. Mahdavi, A. Shafiee, *RSC Adv.* **2015**, *5*, 71297.
[65] L. Ma'mani, S. Miri, M. Mahdavi, S. Bahadorikhalili, E. Lotfi, A. Foroumadi, A. Shafiee, *RSC Adv.* **2014**, *4*, 48613.
[66] L. Ma'mani, S. Nikzad, H. Kheiri-Manjili, S. Al-Musawi, M. Saeedi, S. Askarlou, A. Foroumadi, A. Shafiee, *Eur. J. Med. Chem.* **2014**, *18*, 646.
[67] Z. Liu, X. Wang, Z. Luo, M. Huo, J. Wu, H. Huo, W. Yang, *PLoS ONE* **2015**, *10*, e0143819.
[68] X. Yang, C. Chen, J. Li, G. Zhao, X. Ren, X. Wang, *RSC Adv.* **2012**, *2*, 8821.
[69] M. L. Bode, D. Gravestock, S. S. Moleele, C. W. van der Westhuyzen, S. C. Pelly, P. A. Steenkamp, H. C. Hoppe, T. Khan, L. A. Nkabinde, *Bioorg. Med. Chem.* **2011**, *19*, 4227.

SUPPORTING INFORMATION

Additional supporting information may be found online in the Supporting Information section at the end of this article.

How to cite this article: Bahadorikhalili S, Malek K, Mahdavi M. Efficient One Pot Synthesis of Phenylimidazo[1,2-*a*]pyridine Derivatives using Multifunctional Copper Catalyst Supported on β-Cyclodextrin Functionalized Magnetic Graphene oxide. *Appl Organomet Chem*. 2020;e5913. https://doi.org/10.1002/aoc.5913